Catalysis Today 145 (2009) 220–226

Contents lists available at ScienceDirect

Catalysis Today

journal homepage: www.elsevier.com/locate/cattod

The ID03 surface diffraction beamline for *in-situ* and real-time X-ray investigations of catalytic reactions at surfaces

O. Balmes [a,*], R. van Rijn [a,b], D. Wermeille [a], A. Resta [a], L. Petit [a], H. Isern [a], T. Dufrane [a], R. Felici [a]

[a] *The European Synchrotron Radiation Facility, BP 220, F-38043 Grenoble Cedex 9, France*
[b] *Kamerlingh Onnes Laboratory, Leiden University, P.O. Box 9504, 2300 RA Leiden, The Netherlands*

ARTICLE INFO

Keywords:
Catalysis
Surface X-ray diffraction
In-situ methods
Time resolved
CO oxidation

ABSTRACT

In this article, we present the current capabilities of the ID03 surface diffraction beamline for the characterisation of catalytic surfaces under reaction. The weak interaction of X-rays with matter makes it possible to design reactor set-ups which can sustain high temperatures and atmospheric pressures while probing the sample reactivity, structure and morphology with surface sensitive X-ray techniques. A few examples are presented as an illustration of the current capabilities.

1. Introduction

In heterogeneous catalysis the catalyst and reactants are in different phases. Commonly the catalyst is a solid and the reactants are in gaseous or liquid phase. The catalyst speeds up a reaction by providing a specific reaction pathway without being consumed. Typical catalysts are metals and metal-oxides whose catalytic properties have often been discovered empirically. The optimization of catalysts has often been hampered by the lack of fundamental knowledge about the inner workings of a catalyst on the atomic scale. Therefore a large part of the research in catalysis has been dedicated to the understanding of the reaction mechanisms and role of the catalyst's surface. In this respect, surface science played an important role from a very early stage [1]. For practical reasons, surface science started largely as a science relying heavily on ultra high vacuum (UHV) conditions. In fact, many surface science techniques used in the laboratory are based on the use of electron or atom beams, which require very low pressures to operate.

As a result, the typical approach for understanding the catalytic properties of metal surfaces has been based on studies performed under UHV conditions. The adsorption geometries of several molecules, together with their dissociation pathways, have been determined and reaction pathways have been proposed [2].

The limitation of this approach is the following: the formation of a certain structure with a certain free energy involves overcoming a kinetic barrier. The most energetically favourable structure might not form at low temperatures and low pressures, because, at these conditions, the kinetic formation barrier is much larger than kT. The system will show a surface structure with a low kinetic barrier which may not be the thermodynamic equilibrium [3]. This is the reason for the existence of the so-called temperature and pressure gap between the reaction pathways determined at low pressure and relative low temperatures, and the real working conditions of a catalyst operating at pressures of several tens of bars and at temperatures of several hundred degrees centigrade.

In contrast to electrons and atoms, which have strong interacting potential with matter, X-rays interactions are relatively weak resulting in a negligible attenuation during the transmission through gases at atmospheric or higher pressures. This makes it possible to perform surface X-ray experiments *in-situ* at atmospheric or even higher pressures during catalytic reactions. Relating the structure and morphology of the catalyst surface with its catalytic activity is thus possible provided the walls of the reactor are made of X-ray transparent material.

The ID03 surface diffraction beamline at the ESRF has always been at the forefront of this field. A relatively small volume batch reactor, with a 360° Be window, has been used for simultaneous determination of the surface structure and the gas composition using a quadrupole mass spectrometer (at pressures up to 2 bar and temperatures up to 650 °C).

In this article we briefly describe the X-ray techniques and instrumentation used for the determination of surface structures and morphologies. We also report on recent results obtained using both the batch reactor and a new flow reactor with a much smaller volume and in which the gas composition can be adjusted resulting in a better control of the catalytic reaction conditions.

2. Theoretical background

With the purpose of correlating the structure and morphology of a surface with its catalytic activity the X-ray based standard techniques are: X-ray reflectivity (XRR), surface X-ray

* Corresponding author. Tel.: +33 476 88 28 54; fax: +33 476 88 23 25.
E-mail address: olivier.balmes@esrf.fr (O. Balmes).

0920-5861/$ – see front matter © 2009 Elsevier B.V. All rights reserved.
doi:10.1016/j.cattod.2009.02.008

diffraction (SXRD) and grazing incidence small angle scattering (GISAXS). These three techniques are complementary and each of them provides a piece of information to help in determining the roughness and morphology of the surface, together with its atomic structure. The surface sensitivity of these techniques relies on the existence of a surface with a low roughness. For a sufficiently flat sample the surface breaks the bulk symmetry. Therefore the diffracted intensity is the convolution of the diffracted intensity of an infinite bulk lattice and a surface. The intensity stemming from the bulk lattice is located at precise positions in the reciprocal space (Bragg peaks) while the signal from the surface extends in between, along the so-called crystal truncation rods (CTRs). The intensity of the surface signal in the CTRs is several orders of magnitude lower than the intensity of the bulk, requiring the use of synchrotron sources in order to make the experiments possible within a reasonable timescale. It is also noteworthy that for SXRD, as a first approximation, the surface intensity does not depend on the angle of incidence except in a region close to the critical angle. However the diffuse signal from the bulk will increase with increasing penetration depth.

X-ray reflectivity is based on the X-ray optical properties of each material. The X-ray refractive index is given by [4]:

$$n = 1 - \frac{1}{2\pi} NZr_0\lambda^2 + \frac{i}{4\pi} N\lambda\mu_a \quad (1)$$

where λ is the X-ray wavelength, N is the numerical density of the material, Z is the atomic number of the material, r_0 is the classical electron radius and μ_a is the absorption coefficient. The imaginary part is typically one or two orders of magnitude smaller than the real component and can usually be neglected in the calculation. The refractive index is always slightly smaller than 1. This implies that for a given angle X-rays will be totally reflected when their wavelength λ is larger than a critical value λ_c. Similarly, for a given λ the X-rays will be reflected for an incidence angle smaller than a critical value α_c, or the vertical exchanged momentum $q_\perp$ is smaller than a critical value, $q_{\perp,c}$.

After having defined the refractive index, the reflectivity versus $q_\perp$ can be calculated using all the classical optics relationships [5]. The reflectivity versus $q_\perp$ and the refractive index versus z are connected by a mathematical relationship, implying that given $n(z)$ is possible to calculate $R(q)$. The inverse process is in general not possible because the measured intensity is a squared modulus and the information of the phase is lost. For $q_\perp \gg q_{\perp,c}$, it can be demonstrated that the reflectivity is given as the square modulus of the Fourier transform of the refractive index expressed as a function of the distance from the surface z [6].

A surface or an interface presents some kind of disorder, which is generally described as roughness. Its main effect is to decrease the reflected intensity. Mathematically this can be represented by an exponential term depending on the average roughness dimension of the surface [7]. In the case of interface roughness this term can be directly included in the algorithm describing a sequence of distinct layers [8].

If the surface presents some kind of disorder, the intensity lost in the specular reflectivity is redistributed in the reciprocal space. Sinha et al. have shown how to calculate the X-ray intensity diffused in the reciprocal space, in the frame of the distorted wave Born approximation, considering the roughness as a small perturbation with respect to the smooth surface [9]. Using their methodology, the description of the scattering from a surface separates in two parts: the first one describing the specular reflection and the second one providing the diffuse scattering.

The work of Sinha et al. has been the basis for the development of the grazing incidence small angle scattering technique providing the mathematical formalism necessary to the evaluation of the scattering from nanometric clusters on smooth surfaces. In this case a full treatment of the problem can be found elsewhere [10]. Neglecting the Vineyard term controlling the X-ray electric field at the surface [11], an approximated formula describing the GISAXS intensity from randomly oriented clusters onto a flat surface is [12]:

$$I(q) \approx S(q)|F(q)|^2 \quad (2)$$

where $F(q)$ is the form factor of the clusters averaged along their possible size distribution and orientation and $S(q)$ is the correlation function describing the average spatial distribution of the clusters on the substrate. From a measurement of the GISAXS intensity, it is possible to determine both the average shape of the clusters and their distribution across the surface [13,14].

While for XRR and GISAXS no assumption is made about the sample's lattice properties, SXRD can only be applied in the case of ordered samples. This technique provides information on the structure of (i) the terminating layers of the ordered substrate lattice, and, if it exists, (ii) of an ordered new structure which can form at the surface. In the first case, the information is contained in the diffracted intensity arising from the termination of the periodic bulk structure. It is located along rods perpendicular to the terminating surface in the reciprocal space and having their origin at the Bragg points of the bulk structure [15]. In the second case, the diffracted intensity is recorded along continuous rods, perpendicular to the surface, with an in-plane periodicity defined by the surface unit cell. If the surface unit cell is undergoing a reconstruction of the bulk cells and, as a result, has in-plane dimensions which are commensurate with the bulk unit cell, the associated rods take the name of fractional order rods (FORs) [16].

A measurement of the intensity of both the CTRs and FORs as a function of the continuous variable l (the reciprocal space coordinate perpendicular to the scattering surface), provides information on (i) the expansion or contraction of the top layers of the substrate, (ii) the substrate roughness and (iii) the in-plane position of all the atoms belonging to the surface unit cell.

To gather sensitivity on a particular atomic species, all of the above techniques can also be coupled with energy scans through absorption edges. In the simplest case, the change in the atomic scattering power at the resonance will make it possible to determine the contribution of a particular atomic species to the scattered intensity. In addition an exact determination of the dependence of the scattered intensity versus the energy shows intensity oscillations. These can be interpreted using the same theoretical approach of EXAFS making it possible to determine the chemical and structural local environment of the resonating element as well [17,18] and [19].

3. Experimental

At the ID03 surface diffraction beamline, all of the above techniques can be applied during an experiment to solve both the structure and the morphology of surfaces.

3.1. Beamline optics

A schematic drawing of the ID03 beamline can be seen in Fig. 1. The beamline source consists of three undulators, two with a period of 35 mm and one with 42 mm, which provide a uniform photon flux in the 6–25 keV energy range. The monochromator is a monolithic channel cut Si(1 1 1) crystal cooled at liquid nitrogen temperature by a cryogenic system able to dissipate the few kW of the white beam power. Following the monochromator a cylindrical

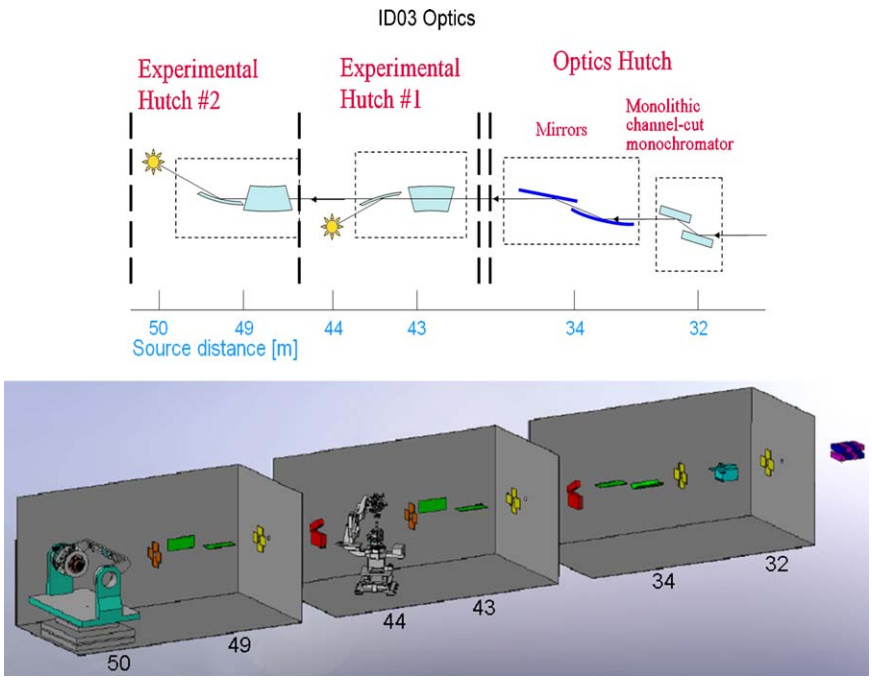

Fig. 1. A schematic view of the optical elements at the ID03 beamline. The beam goes from right to left stemming from the undulators. The optical elements on the beam path are (i) in the optics hutch: channel cut monochromator, cylindrical bendable mirror, second mirror, (ii) in the first experimental hutch: vertical focusing KB mirror, horizontal focusing KB mirror, sample, (iii) in the second experimental hutch: vertical focusing KB mirror, horizontal focusing KB mirror, sample. The numbers below the graph are the distance to the undulators (middle of the straight section).

bendable mirror enables the horizontal and vertical focusing of the beam with a typical focal size of 40×30 ($H \times V$) μm^2 at any position of the two beamline experimental hutches. The angle of incidence of the mirror defines the focal distance for the horizontal focusing, while the bending controls the vertical focusing position. When combining XRR, SXRD and GISAXS, it is crucial to have the possibility of decoupling the horizontal and vertical focusing. For instance, in GISAXS it is preferable to focus at the sample position in the direction perpendicular to the sample surface, and on the 2D detector in the direction parallel to the sample surface. The above optics provides a monochromatic X-ray beam on the sample with a flux exceeding 2×10^{13} ph/s within the whole energy range. Moreover, because of the large vertical acceptance of the optics, energy scans of several hundred eV can be performed without needing to readjust the sample and optical components heights.

Catalysis studies are carried out in the first experimental hutch of the ID03 beamline where a vertical *z*-axis diffractometer is present. This instrument is able to hold special dedicated experimental set-ups with a maximum weight of about 60 kg. The X-ray angle of incidence can be accurately positioned to control either the magnitude of the X-ray electrical field at the surface or the penetration of the X-rays within the sample, which is the main source for the experimental background intensity.

To characterise catalytic processes at surfaces under realistic conditions, we need to have a reactor which merges the capability of clean sample preparation (requiring UHV conditions), with the possibility of exposing the sample to high gas pressures and temperatures where the reactions occur. The possibility of using traditional UHV techniques is crucial in ensuring a reproducible starting point for every sample. The set-ups in use at ID03 enable a traditional preparation of the samples with UHV techniques such as ion bombardment, heat treatment and e-beam deposition. The clean, flat samples can then be characterised with X-ray techniques still under UHV conditions. The subsequent exposure to various pressure or temperature conditions can be done in the same set-up, without exposing the sample to air or transferring it to another set-up. This chain of events ensures that the observed features are neither preparation nor transfer artifacts.

X-ray techniques require (i) as little matter as possible present on the beam path (except for the sample itself) and (ii) this matter, if possible, should have a low atomic number (since interaction of X-rays with matter increases with increasing atomic number). The most common materials used for making X-ray windows are beryllium or plastic films such as Kapton®, with a preference for beryllium in UHV chambers. Another requirement for diffraction experiments is to avoid as far as possible any blocking of the space above the sample surface in order to allow the incoming and outgoing beam to pass at any position of the sample and detector. This imposes geometrical constraints on the experimental set-ups design.

At present three different reactors are available for users' experiments at the ID03 beamline whose characteristics are summarized in Table 1.

3.2. Batch reactor

The high pressure batch reactor (Fig. 2) was developed by Ferrer and co-workers [20]. It consists of a small UHV chamber (pressures down to 10^{-9} mbar) with a large 360° Be window. The turbo pump and other UHV equipment are located above the sample in order to leave a large solid angle above the sample surface for exploring reciprocal space. A leak valve, located in the lower section of the chamber allows for introducing gases. The lower section can be sealed off with a gate valve. An adjustable leak to the top section makes it possible to monitor the composition in the lower section at any pressure through a quadrupole mass spectrometer (Residual Gas Analyzer, RGA). The maximum operating pressure is 2 bar. The sample can be heated under UHV conditions up to 1100 °C, while in oxygen rich conditions the maximum working temperature is about 500 °C. The large volume of about 1 l limits the possibility to study reactions under flow conditions at high pressure.

Table 1
Comparison of the *in-situ* catalysis reactors on ID03 beamline.

	Batch reactor	Batch reactor for harsh conditions	Flow reactor
T_{max}	1100 °C (UHV) 800 °C[a] (2 Atm)	1100 °C (UHV) 800 °C[a] (1 Atm)	1100 °C (UHV) 500 °C[a] (1 Atm)
Deposition	1 evap.	3 evap.	1 evap.
Volume	1 l	2 l	15 cm^3
Window	Beryllium cylinder	Aluminum cylinder	Beryllium dome

[a] Depending on the gas composition.

3.3. Batch reactor for harsh conditions

Based on the design of the batch reactor we have developed a new chamber which can handle corrosive gases (Fig. 3). The 360° X-ray window is made of a 1 mm thick Al cylinder. This imposes the restriction of working at high X-ray energies around 20 keV or above. Contrary to the batch reactor, all the UHV components together with the gas line are located at the lower part of the apparatus. In the top section e-beam evaporators together with an ion gun for sample sputtering can be installed. The technical specifications here are similar to the batch reactor. The sample can be annealed up to 1100 °C under UHV conditions (min pressure 10^{-9} mbar) and heated up to 500–600 °C under operating conditions. The chamber can be used with corrosive gases such as HCl and H_2S. A HCl trap can be mounted on the gas exhaust line of the pump.

3.4. Flow reactor

The flow reactor is an apparatus whose original design stems from the Interface Physics Group of Leiden University (Prof J.W.M. Frenken) and was built through a collaboration between the ESRF

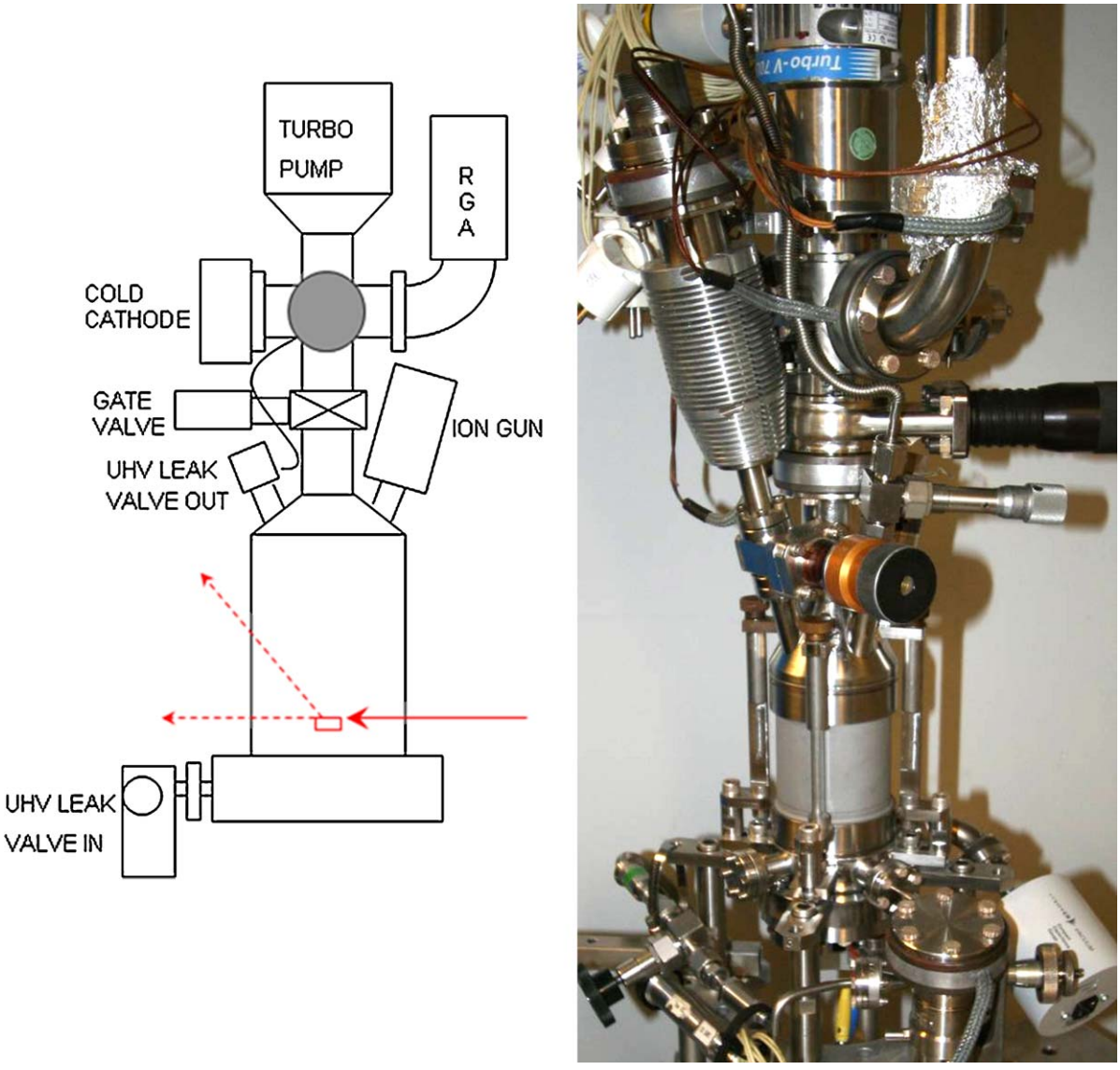

Fig. 2. Left: a schematic drawing of the high pressure batch reactor. The sample is represented as a red rectangle at the bottom. The incoming X-ray beam is represented as a solid red arrow, the outgoing beam is represented as dashed red arrows. Right: a picture of the batch reactor.

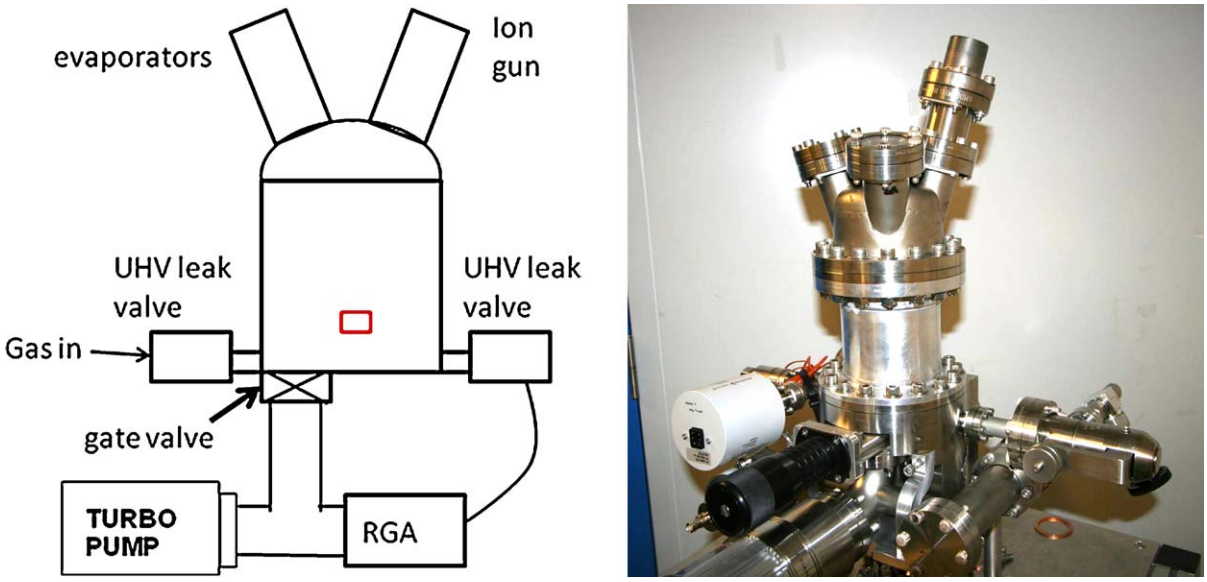

Fig. 3. Left: a schematic drawing of the batch reactor for harsh conditions. The sample is represented as a red rectangle at the bottom. Right: a picture of the reactor.

and Leiden University (see Fig. 4). On the lower part lies the UHV section of the chamber whose upper flange, holding all the UHV tools such as ion sputter gun and e-beam evaporators, can be moved up and down with respect to the sample position. When the top part of the chamber is up, the sample is under UHV conditions (base pressure $\sim 10^{-9}$ mbar) and the sample surface can be prepared using standard UHV techniques. When the top part is down, the region around the sample is sealed off and the small reactor volume (about 15 ml) is isolated from the UHV part of the set-up. Gas can flow in and out of the reactor through two capillaries. The characteristic refresh time of the reactor is in the order of 20 s, allowing fast composition changes to be monitored. The bottom section remains pumped to UHV conditions at all times and an adjustable leak from the reactor allows the RGA to monitor the gas composition in real time.

3.5. Sample and sample environment

Several requirements have to be fulfilled by the sample to ensure a successful experiment. For surface X-ray diffraction, GISAXS and reflectivity, the sample surface must be optically flat, presenting a mirror-like finish. This is usually ensured by using suitably polished surfaces (many materials are commercially available). The sample should be a single crystal with a known orientation and minimal miscut. Polycrystalline or amorphous materials may be used as well, however the lack of a well-defined crystalline lattice will limit the amount of information which can be obtained, in particular for SXRD. The sample may also be used as a substrate for deposition of nanoparticles or layers from evaporators, with similar requirements on the surface finish and roughness.

Inside the reactors, the sample is mounted directly onto the heater. The geometry is the same in all three reactors and therefore, the same sample can be mounted in any of them. The heater is a resistive carbon circuit encapsulated in a boron nitride coating. The geometry of the sample mounting can be seen on Fig. 5. The ideal sample shape for this mounting is a disc of about 10 mm diameter and 2 mm thickness, with a groove or a step (hat-shaped sample) on its side. Only the top side needs to be polished. The groove or step is used to fix the sample firmly to the heater with a clip. It is essential that the material of the clip is compatible with the type of conditions required by the experiment and that it is not catalytically active under those conditions. Two materials are used on a regular basis, tantalum for oxidative environments and molybdenum for hydrogen-rich environments. Tungsten can also

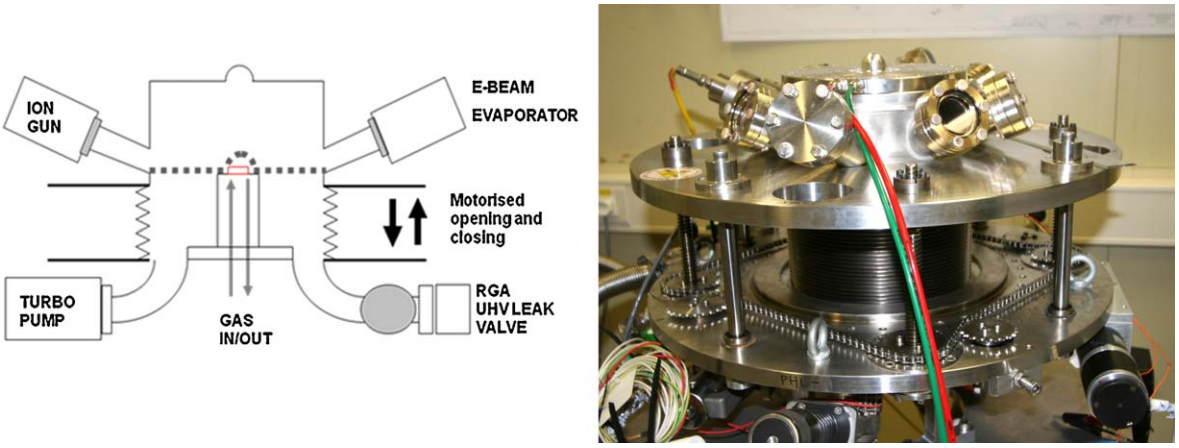

Fig. 4. Left: a schematic drawing of the flow reactor. The sample is represented as a red rectangle. Right: a picture of the flow reactor.

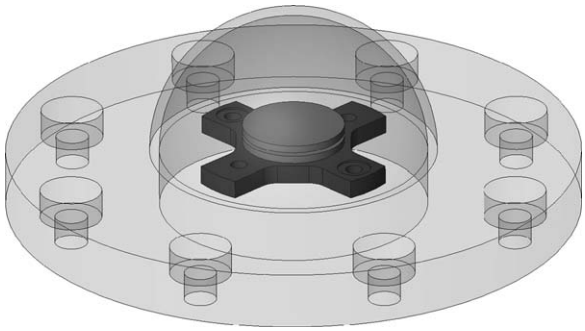

Fig. 5. A schematic view of the sample heater (dark grey) with a sample on it (grey). The sample diameter is 10 mm. The beryllium dome of the flow chamber is shown in light grey.

be used in some cases, however its difficult workability makes it less desirable. It is possible to study smaller samples as well, using purpose-designed holding pieces. A successful experiment was realised with a sample surface only 200 μm × 200 μm large. The temperature of the sample is measured with a Chromel/Alumel thermocouple pinched between the sample and holding clip. When CO is used, the nickel contained in the Chromel and Alumel reacts and forms volatile carbonyls. In this case, a Tungsten/Rhenium thermocouple is used instead.

The same gases can be used in the batch reactor and the flow reactor and are limited to non-corrosive gases, for example H_2, N_2, O_2, CO, NO, CH_4, C_2H_2. Great care must be taken of not using explosive mixtures or conditions which could destroy the beryllium window. The accepted gases are also limited to those which would not cause permanent modification of the set-up, e.g. by deposition of a chemical species at places other than the sample itself. The harsh conditions reactor can be used for corrosive gases such as HCl or sulfur-containing gases.

3.6. Remote controlled gas system

An important addition to the flow reactor set-up is a remote controlled gas system which can be used to change gases via the beamline control software (SPEC) which also controls the diffractometer. This gas system replaces the manual set-up previously used. The system has an array of four mass-flow controllers at the gas inlet which allows mixing exact proportions of the desired gases. It also includes a low dead volume gas line to the reactor and a pressure controller placed after the reactor to adjust the pressure. This new system has substantial advantages compared to the previously used manual set-up: (i) the first 30 s after a gas change are now accessible (they were always lost with the manual system because of the safety procedures in place for closing the experimental hutches); (ii) the on-line mixing of gases in precise proportions is now possible (within the range of the mass-flow controllers); (iii) the total pressure can be kept constant; (iv) it is possible to write and execute macros combining gas changes and diffractometer scans.

4. Results

The ID03 surface diffraction beamline and its instrumentation have been used to study several problems in surface catalysis. Among them, the oxidation of carbon monoxide is a school reaction for catalysis, which happens at the surface of a few transition metals in a wide range of pressures and temperatures. This reaction also has practical and important applications and the platinum group metals are used for catalysing this reaction on a large scale, for example in the exhaust system of combustion engines.

The batch reactor has been extensively used to determine the structure and the morphology of the surface of Pt [21], Pd [3], Ru [22], Rh [23] and some of their alloys [24] under reaction conditions. All of these metals show a clear trend: the rate of production of carbon dioxide strongly depends on the surface structure. The general observation is that under given reaction conditions, an oxide appears at the surface whose presence is well correlated with a simultaneous increase in carbon dioxide production rate, as measured by the mass spectrometer.

The presence of oxide is detected from the observation of diffraction peaks or rods indicating the existence of a periodic structure. In principle, amounts as low as a single layer or nanoparticles can be detected. The well-defined lattice constant and orientation of this structure with respect to the metal correspond to defined oxide phases of the metal.

During an *in-situ* experiment with a time resolution in the order of 1 s or less, it is practically impossible to monitor a large portion of the reciprocal space in order to correlate the presence of an unknown ordered surface phase with its catalytic activity. This is because the measurement of intensities in the reciprocal space requires movement of both the detector and the sample. Particular experimental set-ups using X-rays at very high energy (about 100 keV or higher) coupled with 2D detectors, or the use of white beam with energy dispersive techniques, allow users to probe a large portion of reciprocal space, keeping the detector fixed. However, a rotation of the sample around the surface normal is always necessary when no plane in reciprocal space can be found, normal to the sample surface, which includes reflections from both the catalytic active phase and the substrate.

As the full determination of surface structures is very time consuming, it is often advantageous, for time resolution-critical observations, to focus attention on a particular point in the reciprocal space characteristic of a certain known surface structure. In this manner we can dedicate the beamtime to the interplay between structure and reactivity.

An exception to this general rule is the work of Ackermann [3,21] dealing with the CO oxidation reactivity of the Pt(1 1 1). In this case the authors observed an increase in the reaction rate due to an unknown oxide phase which has a commensurate structure with the bulk metal phase.

The detection of an oxide or surface oxide layer is possible down to sub-monolayer coverage, provided the oxide structure is periodic. In fact it is often not possible to prove by diffraction alone that a layer is fully covering, as it may give rise to a diffraction pattern already at partial coverage. The thickness of the oxide layer can be determined either from a reflectivity measurement or from fitting the crystal truncation rods. However, an amorphous structure will be more difficult to identify uniquely. We therefore speak of the presence of an oxide when a periodic structure with an appropriate lattice constant, and possibly orientation, can be observed.

Recent results obtained in the batch chamber can be read in this edition of *Catalysis Today* (Over et al.) [25]. The role of RuO_2 for the oxidation of carbon monoxide was investigated in detail under reaction conditions. The results show that the active phase is stable only under reaction conditions and a clear structure–activity relationship, calling for *in-situ* characterisation. It was demonstrated that the oxidic surface was more active than the non-oxidic surface for this particular reaction.

Another different reaction that has been investigated is the hydrogenation of carbon monoxide to methane, over a nickel catalyst. It was shown that a layer of carbide built-up at the surface at high pressure and temperature, however this could not be conclusively reproduced during the reaction [26].

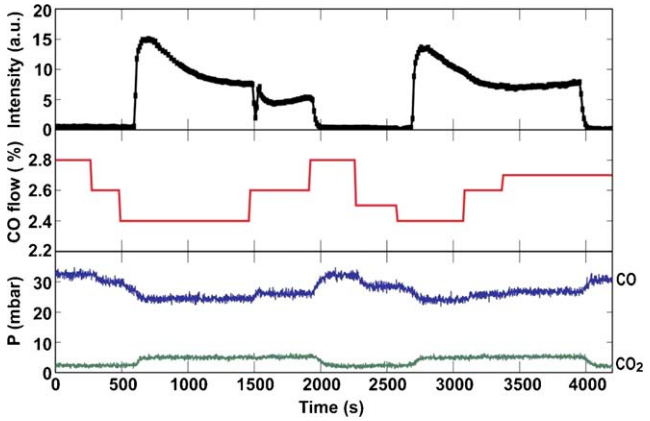

Fig. 6. An example of simultaneous observation of X-ray intensity on a palladium oxide peak (black) and gas composition (CO in blue and CO_2 in green) during gas flow compositional changes (CO mass-flow controller value in red (as a percentage of total flow, here 50 mbar l/min). The sample temperature is 183 °C. An increase in CO_2 production rate can be observed simultaneous to the presence of oxide. (For interpretation of the references to color in this figure legend, the reader is referred to the web version of the article.)

The first results from the flow chamber were presented at the ECOSS 25 conference in Liverpool and the ICSOS 9 conference in Brazil and will be published elsewhere. The first system studied in this chamber was the CO oxidation over palladium during self-sustained reaction rate oscillations. Here the surface spontaneously switches between oxide covered and bare metal while simultaneously, the reactivity switches from high (oxide) to low (metal). Combined measurements of surface X-ray diffraction and grazing incidence small angle scattering shine new light on the driving force for these reaction oscillations. The possibility to tune the CO/O_2 ratio while observing the palladium oxide position in reciprocal space makes it possible to determine very precisely the conditions of appearance of the oxide. Using a 2D pixel detector, the thickness of the oxide layer can also be observed with a time resolution on the order of a second during the reaction rate oscillations. An example of simultaneous measurement during reaction can be seen in Fig. 6. The integrated intensity (top graph) is related to the volume of oxide diffracting. The CO flow graph (middle) shows the set point of the mass-flow controller. The CO and CO_2 graph (bottom) show when the reactivity is high or low (high resp. low CO_2 pressure). The oxide appears a few seconds after the CO pressure is decreased from 2.6% to 2.4%. The reactivity increases simultaneously as the oxide appears and remains high for as long as the oxide is present. Thanks to the possibility of running automated sequences in the gas composition, a large number of conditions can be explored in a reproducible manner, while observing the diffracted signal or GISAXS with seconds time resolution.

5. Conclusion

Using a range of techniques is beneficial in order to elucidate the structure of catalytic surfaces and the mechanisms governing catalytic reactions. X-ray diffraction brings its own set of capabilities in this field, in particular the highest temperatures or pressures attainable are not inherently limited by the technique itself but rather by the technical constraints of the set-up. One challenge in reaching truly industrial conditions is the development of a sufficiently robust sample environment which still allows the X-ray to travel through without loss of information. Innovative designs therefore allow for breakthroughs. We have briefly presented here the three reactors in use at ID03-surface diffraction beamline at ESRF. They push the range of accessible temperatures, pressures and gas compositions closer to industrial conditions while probing the surface structure and morphology by surface X-ray techniques.

References

[1] M. Salmeron, G.A. Somorjai, J. Phys. Chem. 86 (1982) 341–350.
[2] T. Engel, G. Ertl, J. Chem. Phys. 69 (1978) 1267.
[3] M.D. Ackermann, PhD Thesis, University of Leiden, The Netherlands, ISBN 978-90-9022489-3.
[4] B.L. Henke, E.M. Gullikson, J.C. Davis, Atomic Data and Nuclear Data Tables 54 (July (2)) (1993) 181–342.
[5] M. Born, E. Wolf, Principles of Optics, Cambridge University Press, Cambridge, UK, 1999.
[6] R. Jacobsson, in: E. Wolf (Ed.), Progress in Optics, North-Holland, Amsterdam, 1966.
[7] L. Nevot, P. Croce, Phys. Appl. 15 (1980) 761.
[8] J. Penfold, R.K. Thomas, J. Phys.: Condens. Matter 2 (1990) 1369–1412.
[9] S.K. Sinha Sirota, E.B. Garott, S. Stanley, Phys. Rev. B 38 (1988) 2297.
[10] R. Lazzari, J. Appl. Cryst. 35 (2002) 406–421.
[11] G.H. Vineyard, Phys. Rev. B 26 (1982) 4146–4159.
[12] M.V.R. Murty, T. Curcic, A. Judy, B.H. Cooper, A.R. Woll, J.D. Brock, S. Kycia, R.L. Headrick, Phys. Rev. B 60 (1999) 16956.
[13] G. Renaud, R. Lazzari, C. Revenant, A. Barbier, M. Noblet, O. Ulrich, F. Leroy, J. Jupille, Y. Borensztein, C.R. Henry, J.-P. Deville, F. Scheurer, J. Mane-Mane, O. Fruchart, Science 300 (2003) 1416.
[14] D.-M. Smilgies, P. Busch, C.M. Papadakis, D. Posselt, Synchr. Rad. News 15 (2002) 35.
[15] I.K. Robinson, Phys. Rev. B 33 (1986) 3830–3836.
[16] R. Feidenhans'l, Surf. Sci. Reports 10 (1989) 105–188.
[17] H. Stragier, J.O. Cross, J.J. Rehr, L.B. Sorensen, C.E. Bouldin, J.C. Woicik, Phys. Rev. Lett. 69 (1992) 3064.
[18] M.G. Proietti, H. Renevier, J.L. Hodeau, J. Garcia, J.F. Berar, P. Wolfers, Phys. Rev. B 59 (1999) 5479–5492.
[19] M. Benfatto, R. Felici, Phys. Rev. B 64 (2001) 115410.
[20] P. Bernard, K. Peters, J. Alvarez, S. Ferrer, Rev. Sci. Instrum. 70 (1999) 1478–1480.
[21] M.D. Ackermann, T.M. Pedersen, B.L.M. Hendriksen, O. Robach, S.C. Bobaru, I. Popa, C. Quiros, H. Kim, B. Hammer, S. Ferrer, J.W.M. Frenken, Phys. Rev. Lett. 95 (2005) 255505.
[22] H. Over, O. Balmes, N. Bovet, E. Lundgren, ESRF Highlight 2007, Catal. Today, this edition.
[23] J. Gustafson, R. Westerström, A. Mikkelsen, X. Torrelles, O. Balmes, N. Bovet, J.N. Andersen, C.J. Baddeley, E. Lundgren, Phys. Rev. B 78 (2008) 045423.
[24] R. Westerström, J.G. Wang, M.D. Ackermann, J. Gustafson, A. Resta, A. Mikkelsen, J.N. Andersen, E. Lundgren, O. Balmes, X. Torrelles, J.W.M. Frenken, B. Hammer, J. Phys.: Condens. Matter 20 (2008) 184018.
[25] H. Over, et al., Catal. Today, this edition.
[26] M. Ackermann, O. Robach, C. Walker, C. Quiros, H. Isern, S. Ferrer, Surf. Sci. 557 (2004) 21–30.